Microtechnique: 2025-2026 Master Semester 1
Fundamentals of integrated photonic components

Assignment #6
Fabry-Perot cavity and ring resonator

Problem 1 (Analytical, 20 points):

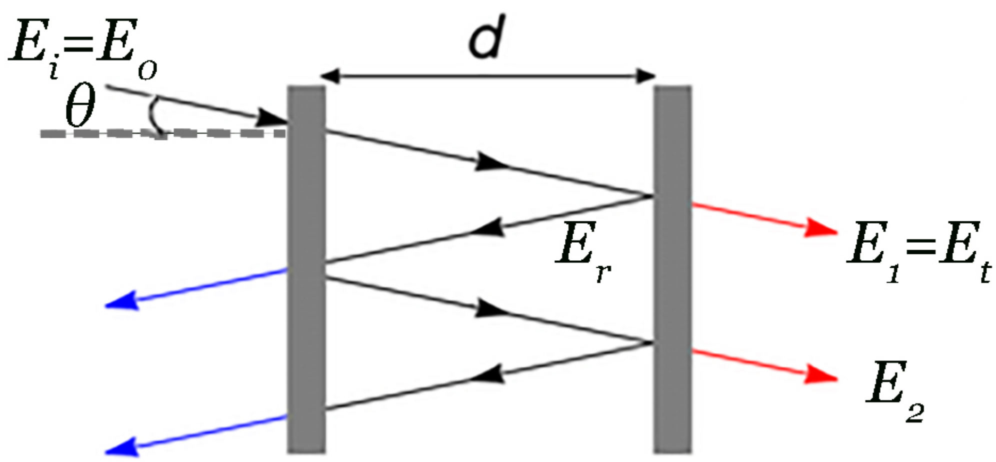

Figure 1: A schematic of Fabry-Pérot

A Fabry-Pérot interferometer consists of two parallel (highly) reflective surfaces separated by a gap of width d and refractive index n, as shown in Figure 1. Each surface has a transmission (t) and reflection (r) coefficient for the electric field wave, such that any time the wave hits the surface we can write:

$$E_t = tE_i \tag{1}$$

$$E_r = rE_i \tag{2}$$

where E_i, E_t, and E_r are the incident, transmitted and reflected electric field, respectively. Consider an external electric field wave E_0 impinging from the left surface with an angle θ.

1. Calculate the total transmitted field E_t^{tot} and the transmittance $T = \frac{I_t}{I_0} = \left(\frac{E_t^{tot}}{E_0}\right)^2$ through the Fabry-Pérot cavity. (5 points)

2. Plot the transmittance as a function of wavelength (between 0.5 and 2 μm) for two different reflectance $R = r^2 = 0.9$ and 0.99, an incident angle of $\theta = 10°$, refractive index of $n = 2.2$, and cavity length of $d = 3\ \mu m$. How do the resonances change for the two different values of R? Explain why. (5 points)

3. With the above parameters (for both R = 0.9 and 0.99), plot the transmittance as a function of frequency. What is the difference between these plots and those vs. wavelength? What is the analytical formula to predict the distance between two peaks in the Transmission as a function of the frequency? (5 points)

4. Plot the transmittance as a function of frequency for two different cavity lengths of $d = 0.5\ \mu m$ and $3\ \mu m$ (incident angle $\theta = 10°$, refractive index $n = 2.2$, and reflectance $R = 0.99$).
From this plot, estimate the quality factor and the Finesse for the mode at the lowest common frequency you can visualize (note that because 3 is multiple of 0.5, both cavities will exhibit a mode at the same frequency). How do Q factor and Finesse of the mode change with these two different cavity lengths? (5 points)

Problem 2 (Simulations, 20 points):

Consider an integrated Fabry-Pérot structure consisting of a ridge waveguide in lithium niobate ($LiNbO_3$) sandwiched between two layers of a material exhibiting higher refractive index. The structure is depicted in Fig. 2. Implement the same structure in CST using the following values for the parameters indicated in the figure:

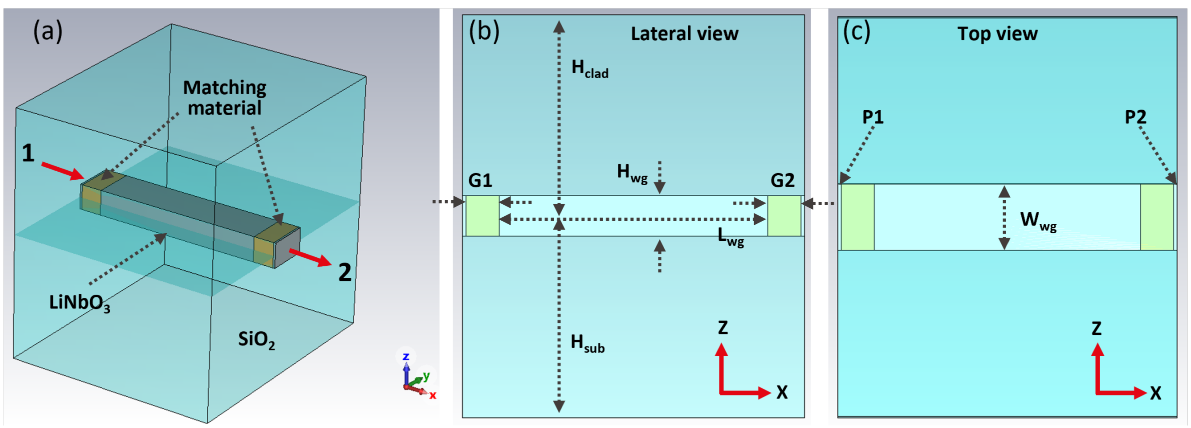

Figure 2: A schematic of Fabry-Pérot interferometer

$P_1 = P_2 = 50\ nm$ (length for the waveguide ports for input (1) and output (2), $LiNbO_3$)
$G_1 = G_2 = 500\ nm$ (length of the matching material with a higher refractive index)
$\lambda = 0.5 - 2\ \mu m$ (wavelength range for the sweep study)
$W_{WG} = 1\ \mu m$ (waveguide width)
$W_{sub} = 6\ \mu m$ (width of the substrate along the y-axis)
$L_{WG} = 4\ \mu m$ (length of the waveguide along the x-axis)
$H_{WG} = 600\ nm$ (height of the waveguide)
$H_{clad} = 3\ \mu m$ (height of the cladding layer)
$H_{sub} = 3\ \mu m$ (height of the substrate)
$n_c = 1.44$ (cladding refractive index, SiO_2)
$n_s = 1.44$ (substrate refractive index, SiO_2)
$n_f = 2.2$ (core refractive index, $LiNbO_3$)
$n_m = 3.48$ (index of the matching layer)

Place a Port1 on the input interface and a Port1 at the output (single mode), add electrical field monitors at 1, 1.55, and 2 μm. Keep the number of your mesh cells less than 2 millions.

1. Compute the effective refractive index of the fundamental mode at the three selected wavelengths 1, 1.55, and 2 μm. Then, launch the mode in the waveguide and show the 2D profile of the electric field at the center

of the structure (x-z plane, absolute value) at the same wavelengths. Plot also S21. Comment and compare the results. (10 points)

2. Extract 1D plot of the electric field (absolute value) at the center of the waveguide (i.e., Y = 0 and Z = 0) along the x-axis at the same wavelengths: 1, 1.55, and 2 μm.
On these plots, select a pair of consecutive nodes. Determine their relative distance ΔL along the waveguide and verify whether the formula $2\Delta L n_{eff} = \lambda$ is valid in all cases. [Note: you can use the values of n_{eff} computed before.] (10 points)

Problem 3 (Simulations, 60 points):

Construct a ring resonator with a bus and a drop waveguides as depicted in Fig. 3 using the following parameters:

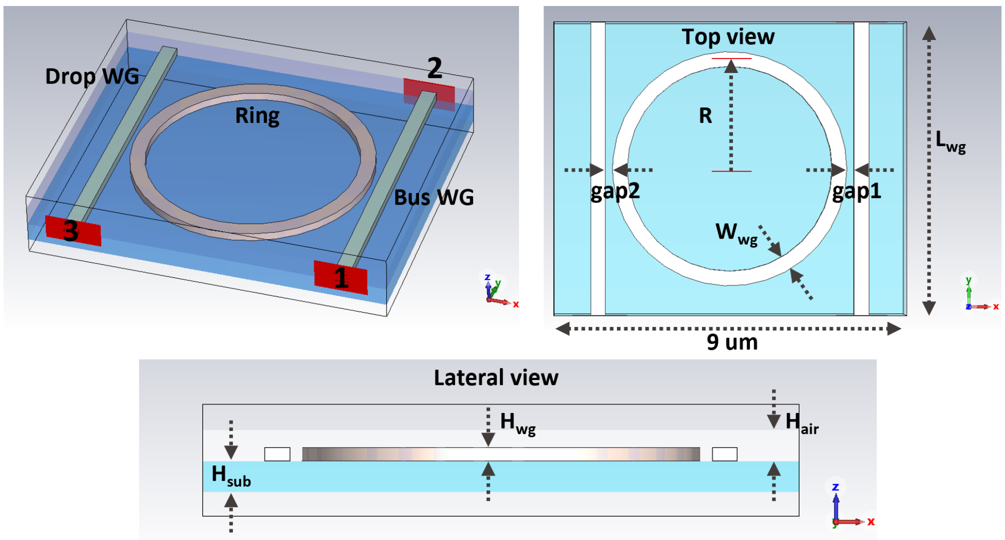

Figure 3: Geometry of the structure, with top and side views of ring, bus and drop waveguides.

- Simulation range: wavelength between 1.5 μm and 1.6 μm
- Geometry:
  - Ring radius 3 μm (the radius is calculated from the center of the ring to the center of the circular waveguide, as shown in Figure 3)
  - W_{WG} = 0.4 μm (same width for ring and waveguides)
  - H_{WG} = 0.22 μm (same height for ring and waveguides)
  - L_{WG} = 8 μm (length of bus and drop waveguides)
  - $gap1$ = 0.2 μm (gap distance between ring and bus waveguide)
  - $gap2$ = 0.2 μm (gap distance between ring and drop waveguide, keep it a separate parameter from gap1)
  - Substrate size: 8 μm x 9 μm
- Material properties:
  - Ring: create a new material with the following modifications:
    Epsilon: 9
    Electric conductivity: 160 S/m (thus this material is lossy)

- Bus and drop waveguides: create another new material with the following modification:
  Epsilon: 9 (lossless)

- Environment: define using "Simulation"-"background"-"Multiple layers"
  - Substrate layer: height 0.5 µm, new material "SiO2" with Epsilon = $n_{SiO_2}^2 = 1.45^2$
  - Cladding layer: height 0.5 µm, material "Air"

- Ports: create three single-mode ports. Refer to Figure 3: restrict Port1 and Port 2 around the input and output of the bus waveguide, respectively. Finally, restrict Port3 around the output of the drop waveguide (on the same side of the input of the bus). **Important: use parameters to define the extension of the ports to be sure they are always centered around the waveguides. Use a width along X of around 1.5** μm **and a height along Z of 0.7** μm **(you can restrict the ports from Z = -0.3 and Z = 0.4).**

- Mesh size: the mesh should be fine enough to resolve the narrow gap between the ring and the waveguides. Suggested mesh size: keep the standard 15 cells per wavelength and 20 cells per max model box edge (total mesh cells ~ 1.6-1.7 million).

Problem:

1. Run the simulation launching only the mode in Port1 as an input (using time domain solver with -40 dB accuracy) and plot the transmission spectra S21 and S31. From the S21 curve, estimate the following parameters for the mode close to 195 THz: Q factor and Finesse. (15 points)

2. Add two E-field monitors, one at the resonance frequency you found above, and the other shifted by 1.5 THz (off-resonance), then run the simulation again. Plot the X-Y view of the E_{abs} and E_x fields for the two frequencies. Observe the evanescent coupling from the bus waveguide to the ring and the field distribution in the system. Comment on your findings. (10 points)

3. Reduce the gap1 distance to find critical coupling (dip<-20 dB) for the mode you analyzed before. **Suggested sweeping range for the gap: from 0.2** μm **down to 0.05** μm **with a step size of 0.05** μm**.** Plot the S21 and S31 curves again and compute Q factor and Finesse for the mode close to 195 THz for in the case of critical coupling. Comment on: for which gap distance over-coupling and under-coupling occur, respectively? Why? Compare the linewidth of the resonance you analyzed by plotting the trend of the FWHM in the four cases. What can you conclude about the various coupling regimes?
   Anticipated total simulation time: 20 min. (15 points)

4. Plot again the X-Y view of the E_{abs} and E_x fields in the critical coupling regime, this time only using the on-resonance monitor. Compare the field distributions in the present case with the one above in question 2 and comment on any difference. (10 points)

5. Keep gap1 equal to the value used to obtain critical coupling. Change the radius of the ring to 2.5 and then 3.5 μm. Plot S21 curves for various radii. Compute again Q factor and Finesse for the mode close to 195 THz for all radii. How do these parameters depend on R? Explain the reason behind these variations. **Suggestion: You can run a single parametric sweep in the same simulation file. CST will automatically skip the case of R = 3** μm **as it was computed before**. Anticipated total simulation time: 10 min. (10 points)

Solution (Analytical):

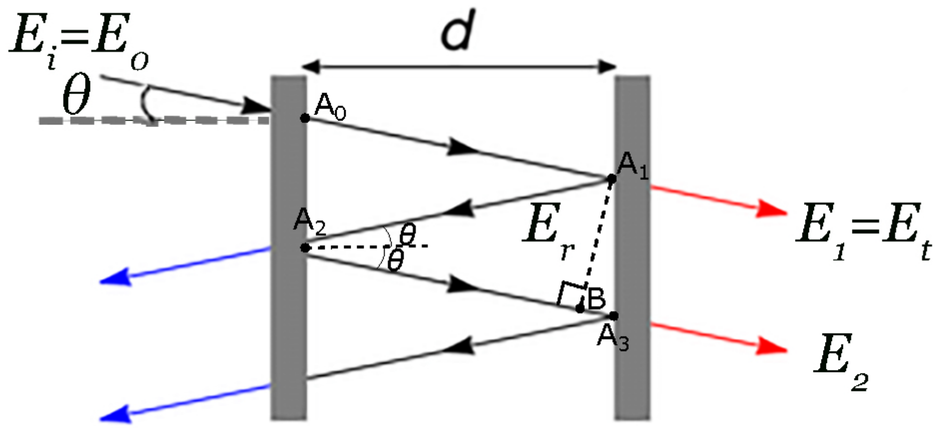

Figure 4: A schematic of Fabry-Pérot

1. In order to form a coherent electric field outside of the FP resonator, each single ray has to be emitted in phase with the other ones. Therefore, let us consider the geometry drawn in Fig. 4. The path difference (p) between wave E_1 and E_2 is $A_1A_2 + A_2B$:

$$\begin{aligned} p &= A_1A_2 + A_2B = A_1A_2 + A_1A_2 \cos 2\theta \\ &= A_1A_2(1 + \cos 2\theta) = 2A_1A_2 \cos^2\theta \\ &= 2d\cos\theta \end{aligned} \tag{3}$$

For any round-trip travel, the displacement between two consecutive rays is always that in Eq. 3. Now, let us write down each component of the total transmitted electric field as a function of E_0 (we take as a reference the field emitted from the point A_1, i.e., E_1):

$$\begin{aligned} E_1 &= t \cdot t \cdot E_0 \\ E_2 &= t \cdot r \cdot r \cdot t \cdot E_0 e^{i\delta} \\ E_3 &= t \cdot r \cdot r \cdot r \cdot r \cdot t \cdot E_0 e^{i2\delta} \\ &.... \\ E_N &= t^2 \cdot r_0^{2(N-1)} e^{i(N-1)\delta} \end{aligned} \tag{4}$$

δ is the phase difference between adjacently transmitted beams, equal to $\delta = nk_0p = \frac{2\pi n}{\lambda}p$.
The total transmitted electric field is:

$$E_t^{tot} = E_1(1 + \alpha + \alpha^2 + ...) = \frac{E_1}{1-\alpha} \tag{5}$$

where $\alpha = r^2e^{i\delta}$. So, the total transmitted electric field is:

$$E_t^{tot} = \frac{t^2E_0}{1 - r^2e^{i\delta}} \tag{6}$$

and the transmittance is:

$$\begin{aligned} T = \frac{I_{tr}}{I_0} &= \frac{E_t^{tot}(E_t^{tot})^*}{E_0E_0^*} \\ &= \frac{t^4}{(1 - r^2cos\delta + ir^2sin\delta)(1 - r^2cos\delta - ir^2sin\delta)} \\ &= \frac{t^4}{1 + r^4 - 2r^2cos\delta} \end{aligned} \tag{7}$$

By considering $\cos\delta = 1 - 2\sin^2\frac{\delta}{2}$ and $t^2 + r^2 = 1$, we can simplify the equation to:

$$T = \frac{1}{1 + (\frac{2r}{1-r^2})^2 \sin^2\frac{\delta}{2}} = \frac{1}{1 + F^2 \sin^2\frac{\delta}{2}} \tag{8}$$

where $F^2 = \frac{4R}{(1-R)^2}$ and $R = r^2$.
2. Now, we plot T as a function of wavelength λ for two different reflectance $R = 0.9$ and 0.99, an incident angle of $\theta = 10°$, a refractive index of $n = 2.2$, and a cavity length of $d = 3\ \mu m$:

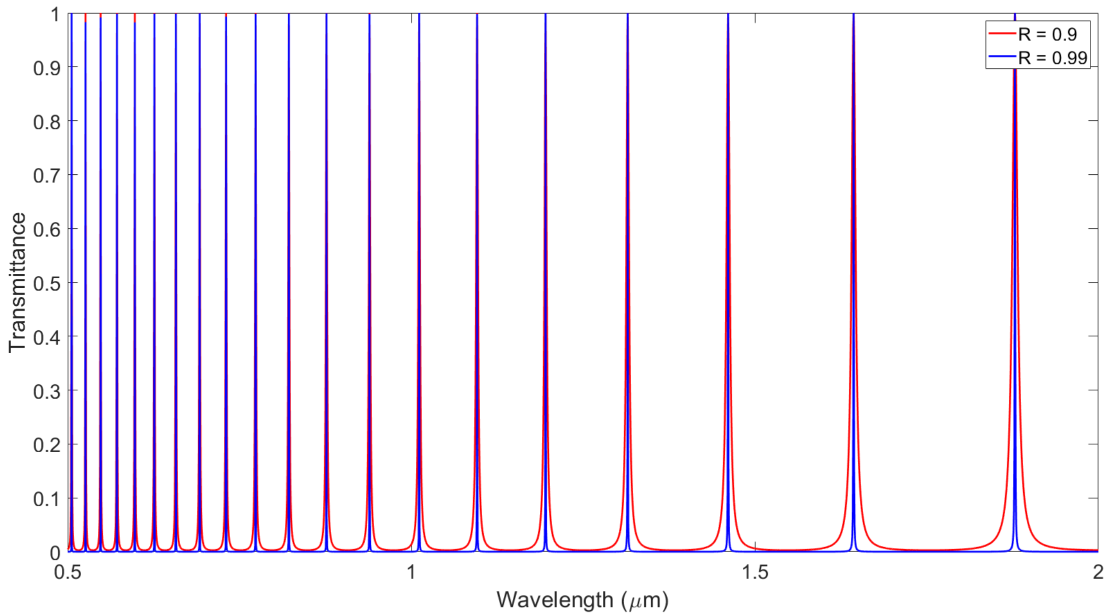

Figure 5: The transmittance as a function of wavelength for two different reflectance $R = r^2 = 0.9$ and 0.99, an incident angle of $\theta = 10°$, refractive index of $n = 2.2$, and cavity length of $d = 3\mu m$.

We can observe that both cavities present resonances for the same wavelength. However, the resonances are narrower when the reflectance increases from 0.9 to 0.99. In fact, with higher reflectance the cavity becomes more selective and only for specific wavelengths the various components of the field interact constructively at the output. Mathematically, we can see that for larger R, F increases, while the FSR remains constant, with a resulting narrower FWHM.

3. If we plot the transmittance for the same parameters as a function of frequency $f = c/\lambda$ (being c the speed of light), we obtain equidistant modes, as shown in Figure 6. The maximum transmittance is obtained when $\frac{\delta}{2} = m\pi$. Hence, $\frac{2n\pi f_m d\cos\theta}{c} = m\pi$ and $f_m = \frac{mc}{2nd\cos\theta}$. The distance between two peaks is the free spectral range (FSR) (i.e., the mode spacing), and it is then equal to:

$$FSR = f_{m+1} - f_m = \frac{c}{2nd\cos\theta} \tag{9}$$

4. The transmittance vs. frequency for two different cavity lengths of $d = 3\mu m$ and $0.5\mu m$ for an incident angle of $\theta = 10°$, a refractive index of $n = 2.2$, and a reflectance of $R = 0.99$ is shown in Fig. 7, while a zoom on the first common mode is shown in Fig. 8.

The quality factor for the first common mode in both cavities is located at $f = 273.58$ THz is:
For $d = 0.5\mu m$:

$$Q = \frac{f}{FWHM} = \frac{273.58}{(273.8 - 273.36)} = 621.77 \tag{10}$$

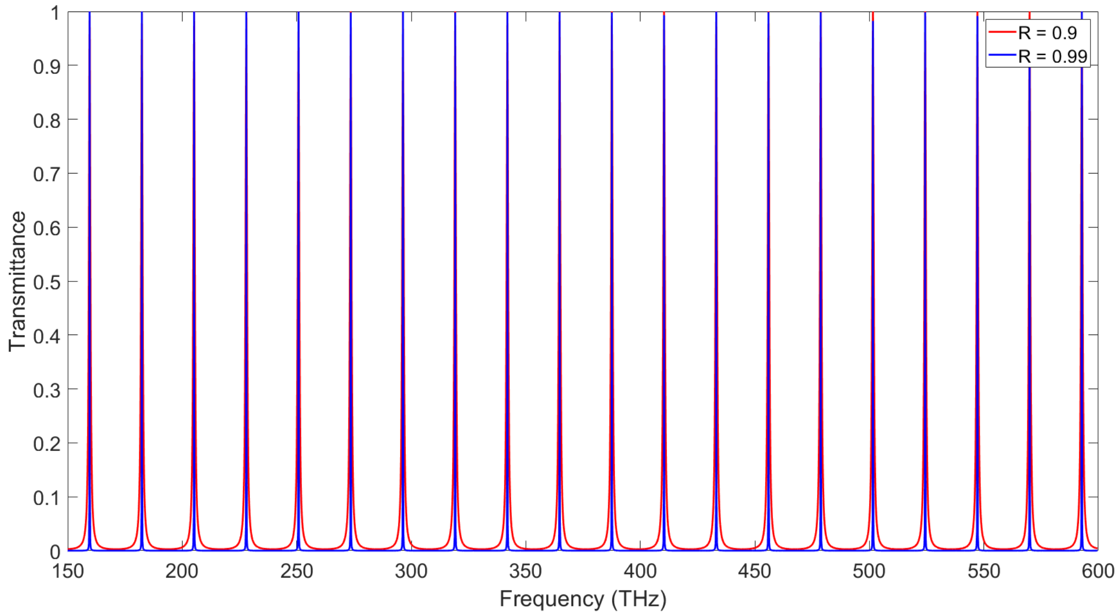

Figure 6: The transmittance as a function of frequency for two different reflectance $R = r^2 = 0.9$ and 0.99, an incident angle of $\theta = 10°$, refractive index of $n = 2.2$, and cavity length of $d = 3\mu m$.

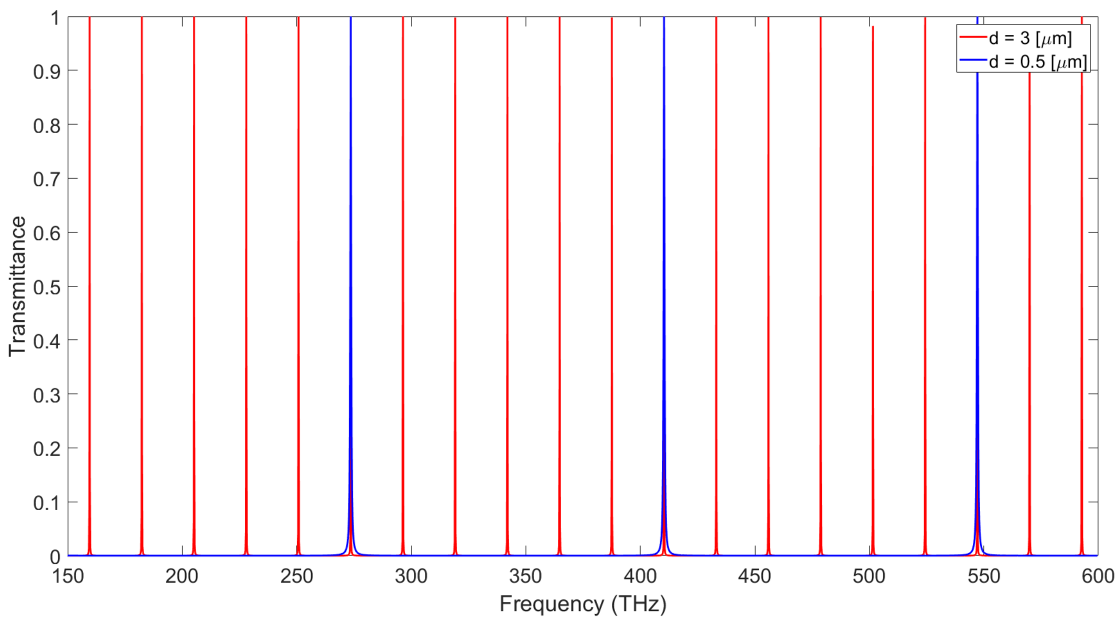

Figure 7: The transmittance as a function of frequency for two different cavity lengths of $d = 3\ \mu m$ and $0.5\mu m$ for an incident angle of $\theta = 10°$, refractive index of $n = 2.2$, and reflectance of $R = 0.9$.

and for $d = 3\mu m$:

$$Q = \frac{f}{FWHM} = \frac{273.58}{(273.62 - 273.54)} = 3419.75 \tag{11}$$

So, the quality factor for the cavity length of $d = 3\mu m$ is more than 5 times larger than that of the cavity with $d = 0.5\mu m$.

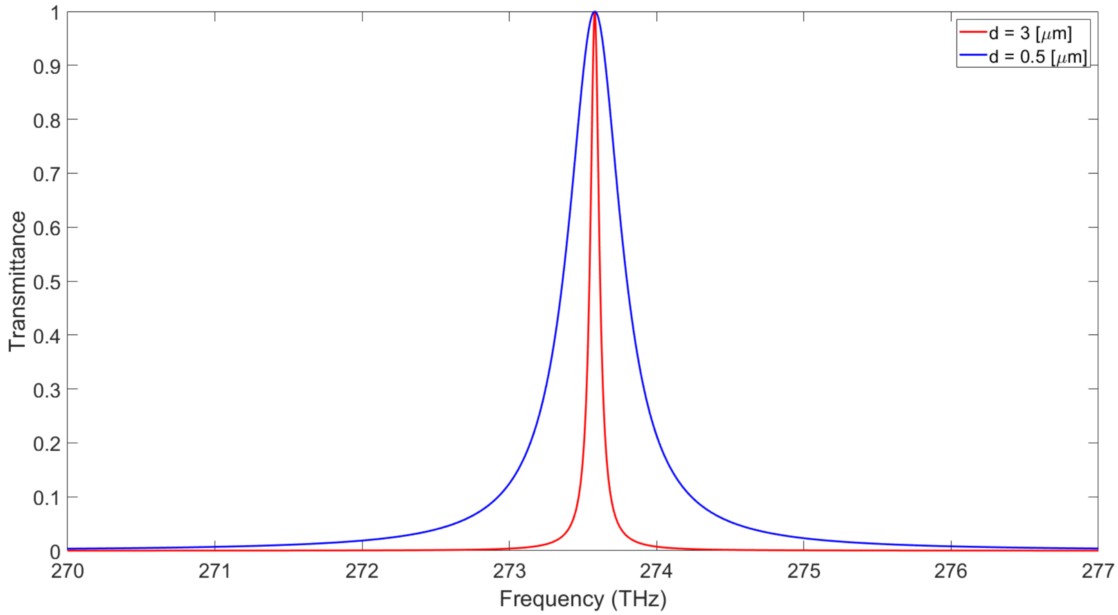

Figure 8: The transmittance as a function of frequency for two different cavity lengths of $d = 3\ \mu m$ and $0.5\mu m$ for an incident angle of $\theta = 10°$, refractive index of $n = 2.2$, and reflectance of $R = 0.9$.

Instead, the finesse F is computed as $F^2 = \frac{\pi\sqrt{R}}{1-R} = 312.58$ and it is independent on the cavity length d.

Solution (Simulation):

1. The effective refractive indices of the fundamental modes are $n_{eff} = 1.908$ at $\lambda = 1$ μm, $n_{eff} = 1.782$ at $\lambda = 1.55$ μm and $n_{eff} = 1.592$ at $\lambda = 2$ μm.
The 2D profile of the electric fields (Absolute value) for the three wavelengths is reported in Fig. 9-11.

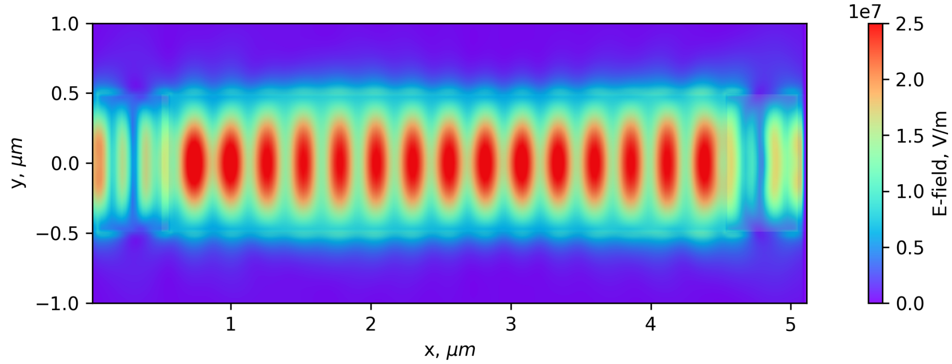

Figure 9: Absolute value of the electric field calculated across the propagation direction. Wavelength is 1 μm.

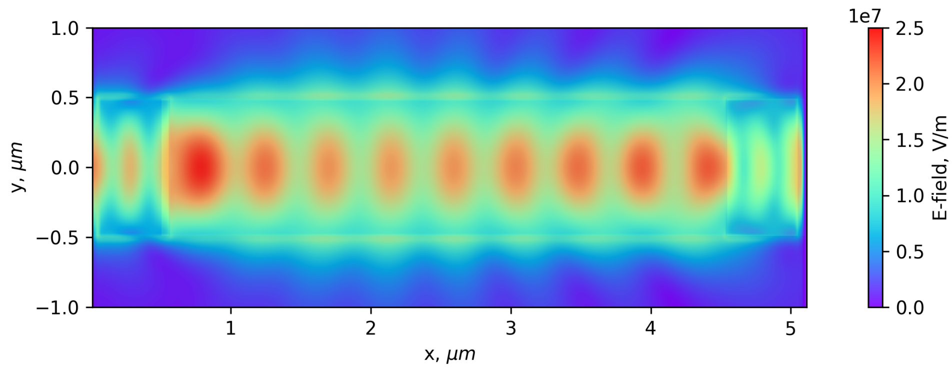

Figure 10: Absolute value of the electric field calculated across the propagation direction. Wavelength is 1.55 μm.

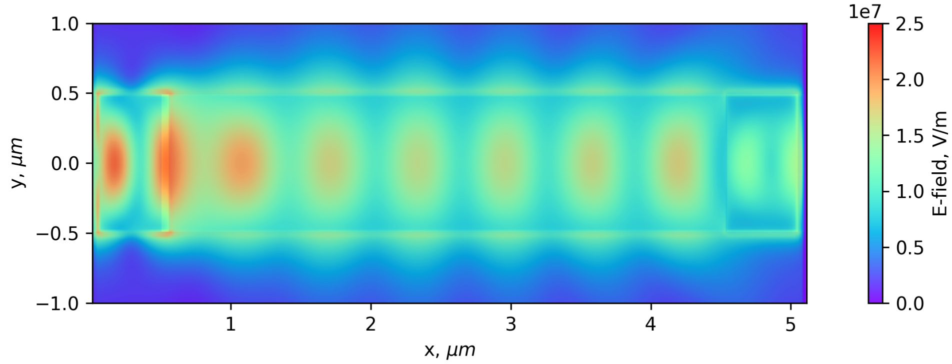

Figure 11: Absolute value of the electric field calculated across the propagation direction. Wavelength is 2 μm.

As expected, the oscillation of the electric field is faster for lower wavelengths and the mode is better confined in the waveguide. When $\lambda = 2\ \mu m$, a larger portion of the field is, in fact, outside the waveguide.

In figure 12 one can see the formation of the resonance modes with local minima in the transmission.

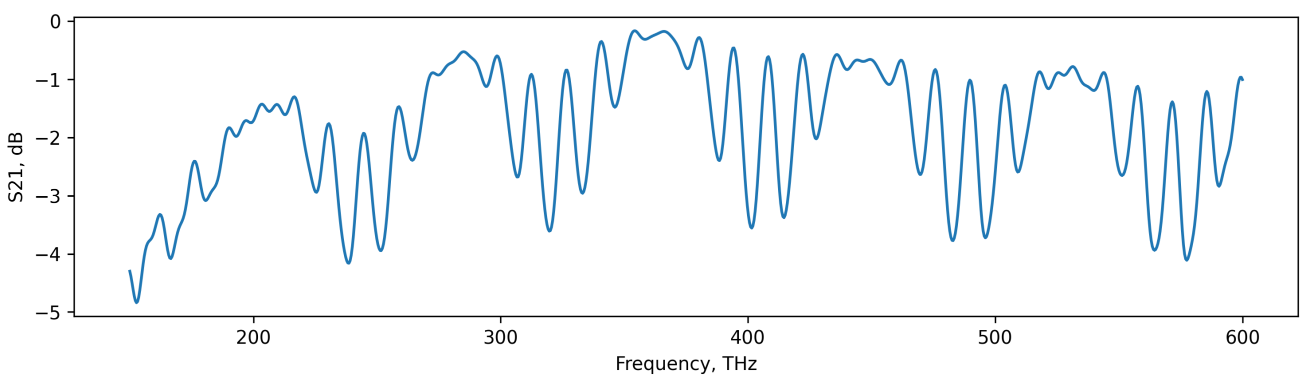

Figure 12: S21 parameter versus frequency

2. The trends of the magnitude of the electric field for the wavelengths of interest are reported in Fig. 13. Using the position of the first two nodes inside the waveguide (between the vertical black lines), we find that: when wavelength is 1 μm, $\lambda = 2n_{1.0}\Delta L = 2 * 1.908 * 0.26\ \mu\text{m} = 0.995\ \mu\text{m}$; when wavelength is 1.55 μm, $\lambda = 2n_{1.55}\Delta L = 2 * 1.713 * 0.45\ \mu\text{m} = 1.553\ \mu\text{m}$; and when wavelength is 2 μm, $\lambda = 2n_2\Delta L = 2 * 1.592 * 0.63\ \mu\text{m} = 2.006\ \mu\text{m}$. Small discrepancies are simply due to the resolution of the mesh.

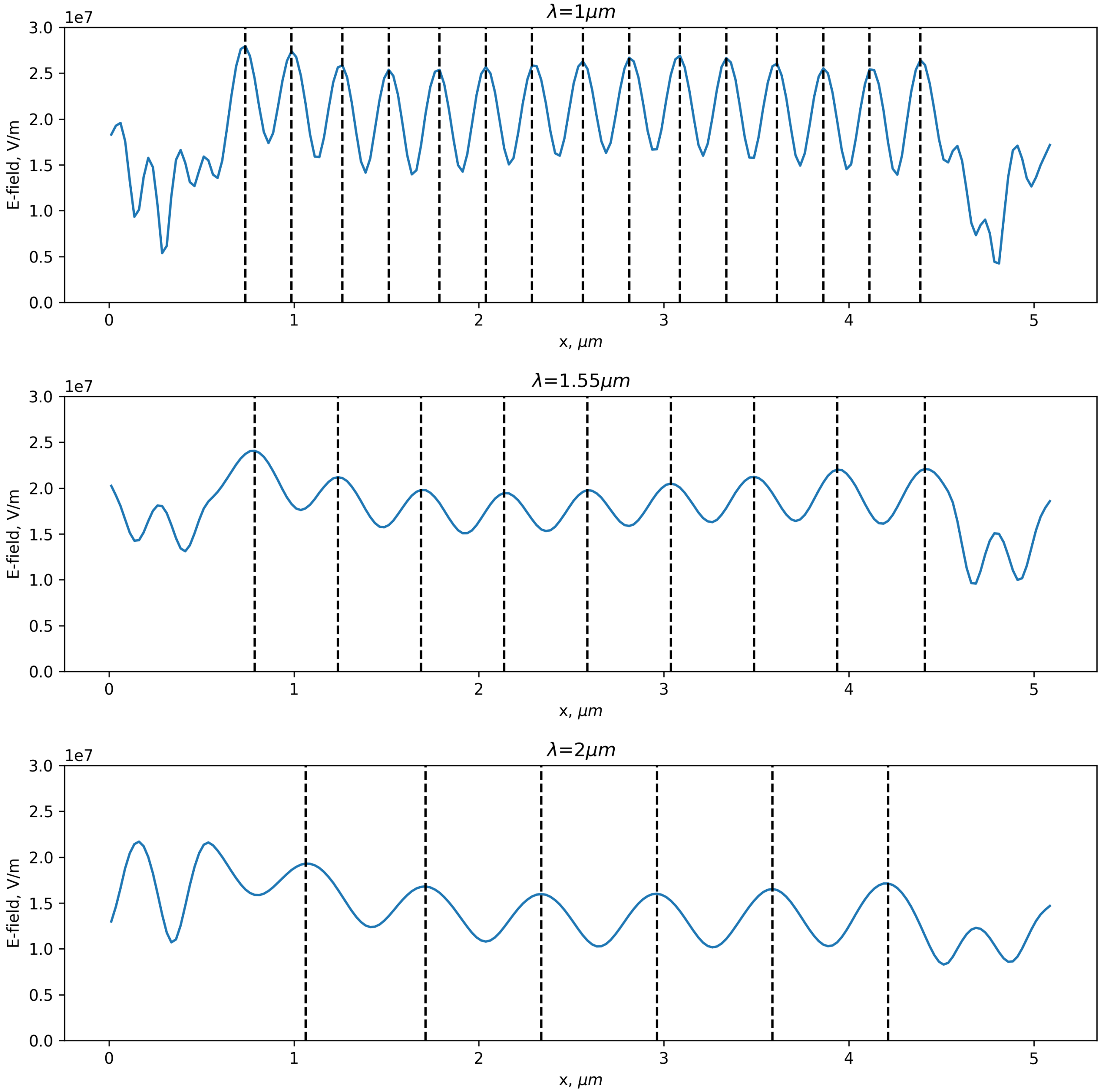

Figure 13: Absolute value of the electric field calculated across the propagation direction, for the wavelengths: $1 - 1.55 - 2\ \mu$m. Dashed lines mark the local maxima needed to compute ΔL.

Solution (Ring resonator simulation):

1. The plot of S_{21} and S_{31} as a function of frequency is reported in Fig. 14, from which we can estimate the Q and finesse as shown below.

We can see that both resonances do not reach -20 dB, meaning that the system is not in critical coupling regime. From the mode around 195 THz, we have $f_{res} = 195.72\,THz$, $FSR = 4.6\,THz$ and $FWHM = 0.79\,THz$. Therefore, we can compute

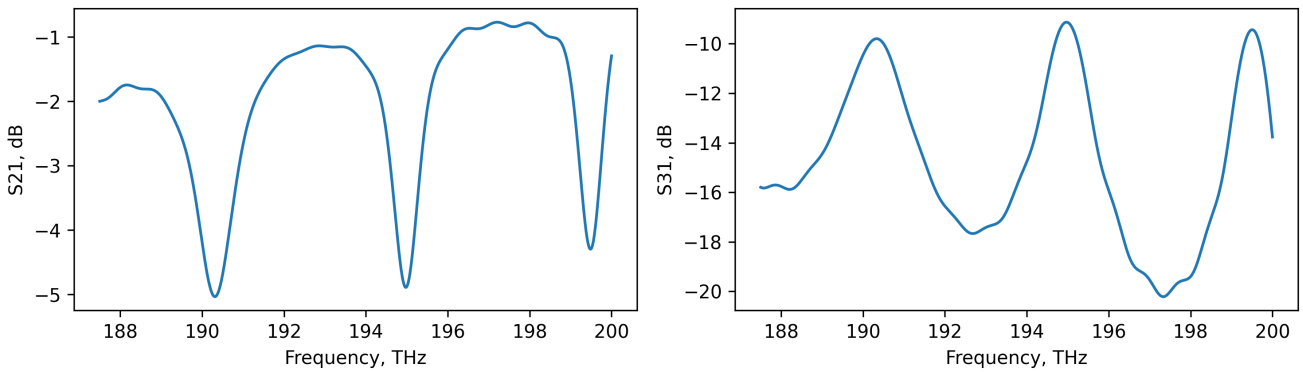

Figure 14: S_{21} and S_{31} as a function of frequency.

$$Q = \frac{f_{res}}{FWHM} \simeq 248 \qquad and \qquad Finesse = \frac{FSR}{FWHM} \simeq 5.82 \tag{12}$$

2. The X-Y view of the E_{abs} and E_x fields for both on- and off-resonance frequencies is reported in Fig. 15.
The field is evanescently coupled from the bus waveguide to the ring resonator in the on-resonance case as shown in the left panels, while the coupling is very weak in the off-resonance case (right panels). The specific field distribution in the ring can provide information about the resonant modes that are excited in the ring and their associated wavelengths. In resonance, the field also couples from the ring to the drop waveguide.

3. The variation of the S21 and S31 spectra with different gap distances from 0.2 to 0.05 μm is shown in Fig. 16.
Critical coupling is obtained when the gap distance is 0.075 μm. The system is in under-coupling regime when the gap is larger (from 0.2 to 0.1 μm), and over coupled when gap is 0.05 μm.

4. The X-Y view of the E_{abs} and E_x fields in the critical coupling regime are reported in Fig. 17.
Comparing the field distributions with those in question 2, we can see that in the critical coupling regime the field is more strongly coupled to the ring. As a consequence, the transmission to the output of the bus waveguide is greatly reduced, while the signal in the drop waveguide increases.

5. The variation of S21 spectra for different ring radii from 2.5 to 3.5μm is shown in Fig. 18.

We can see that the resonance getting worse with changing the radius, meaning that changing the bending losses doesn't improve the critical coupling condition. At the same time we see that with larger R the FSR is decreasing.

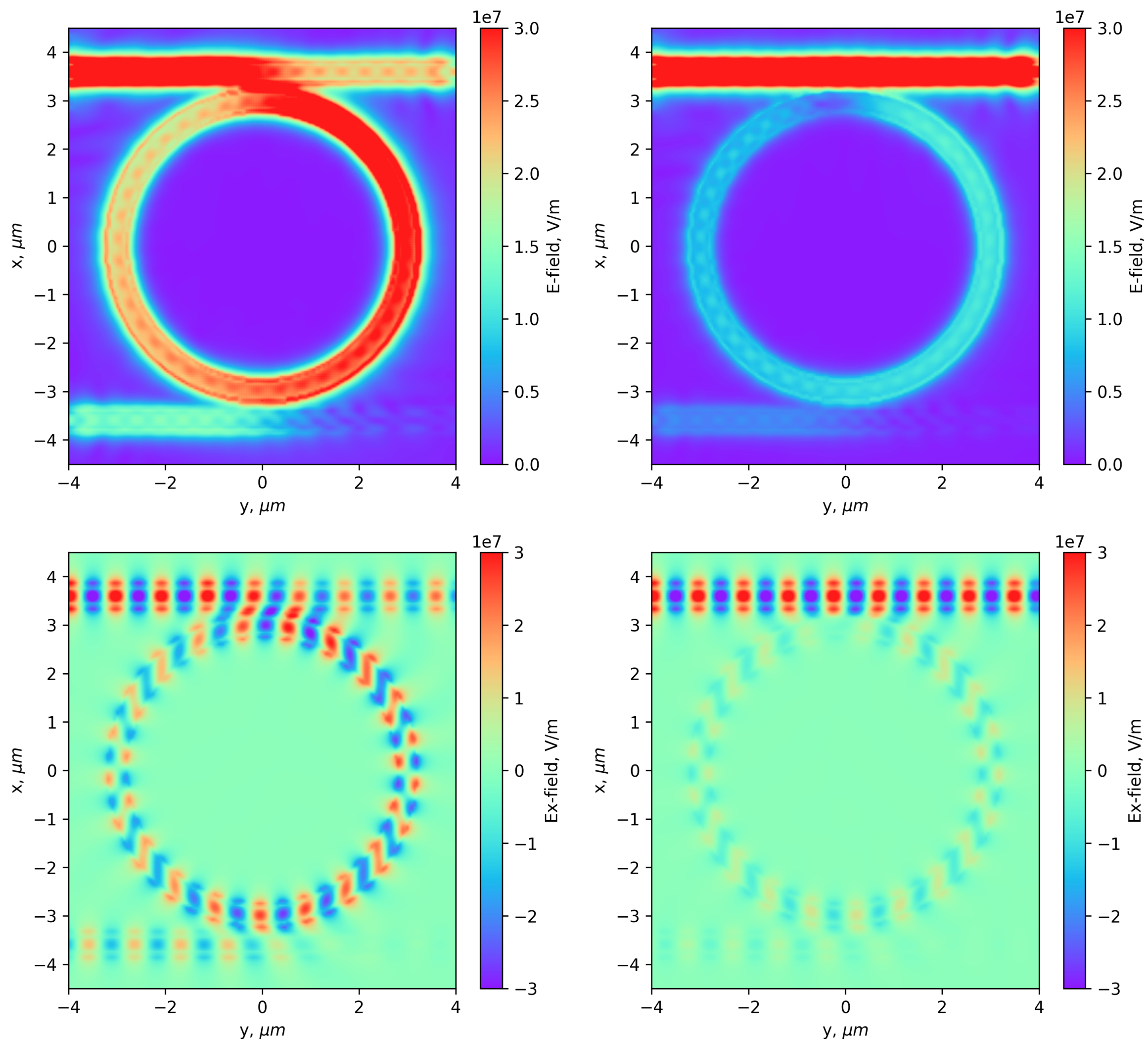

Figure 15: E_{abs} and E_x field distributions when the frequency is on-resonance (left panels) or off-resonance (right panels)

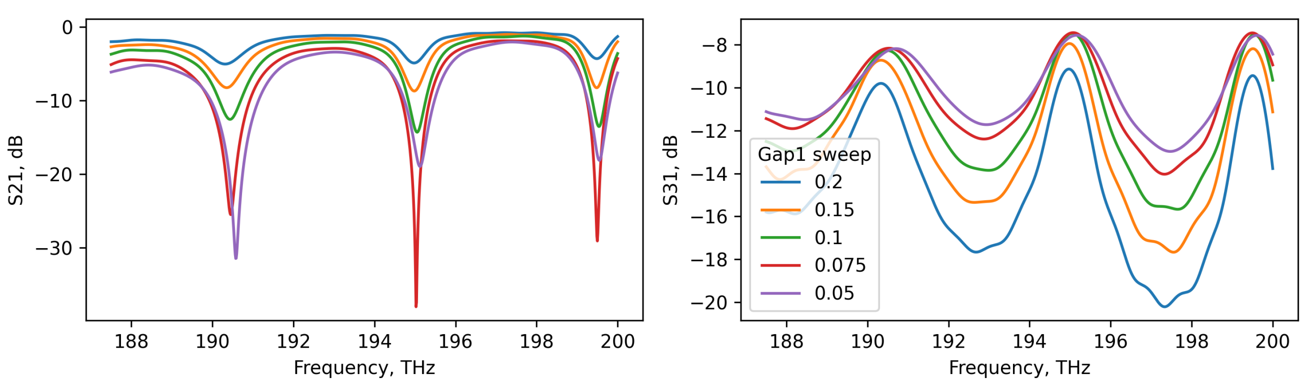

Figure 16: Variation of the S21 and S31 spectra with different gap distances from 0.2 to 0.05 μm

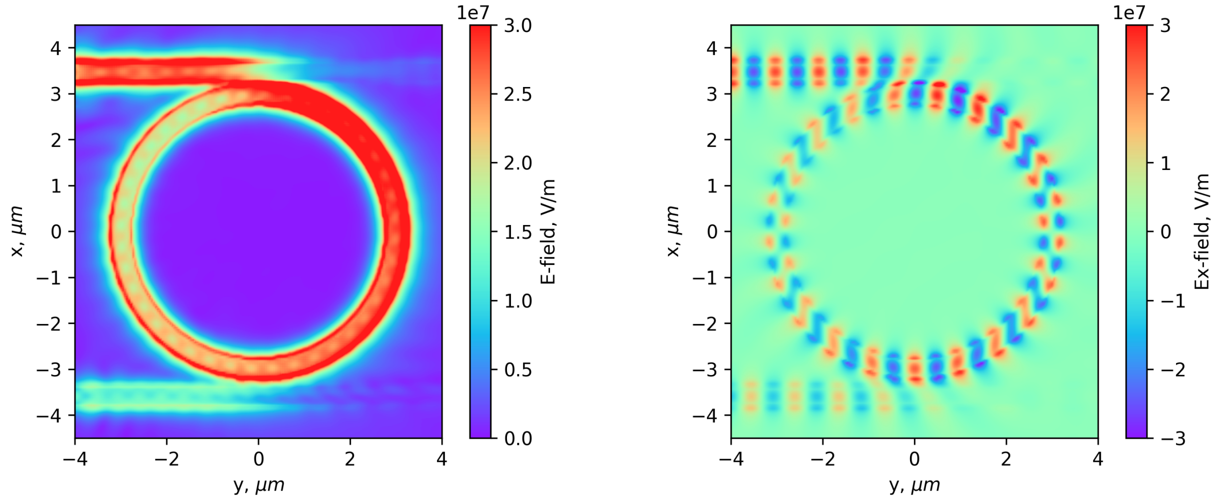

Figure 17: E_{abs} and E_x fields on resonance in the critical coupling regime.

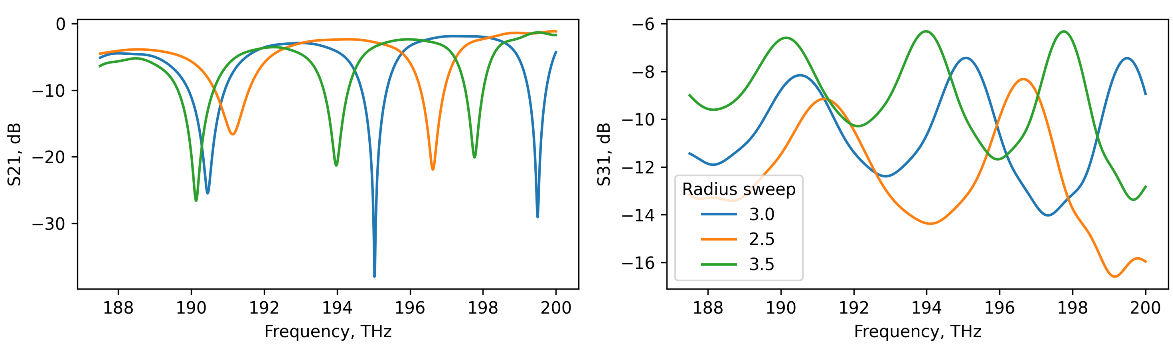

Figure 18: Variation of transmission spectra with different ring radius from 2.5 to 3.5μm